J|A|C|S

A R T I C L E S

High Energy and Quantum Efficiency in Photoinduced Charge Separation

John M. Weber, Matthew T. Rawls, Valerie J. MacKenzie, Bradford R. Limoges, and C. Michael Elliott*

Contribution from the Department of Chemistry, Colorado State University, Fort Collins, Colorado 80523

Received September 11, 2006; E-mail: elliott@lamar.colostate.edu

Abstract: Supramolecular triad assemblies consisting of a central trisbipyridine ruthenium(II) chromophore (C^{2+}) with one or more appended phenothiazine electron donors (D) and a diquat-type electron acceptor (A^{2+}) have been shown to form long-lived photoinduced charge separated states (CSS) with unusually and consistently high quantum efficiency. Up to now, there has been no understanding for why these large efficiencies (often close to unity) are achieved across this entire class of triads when other, seemingly similar systems are often much less efficient. In the present study, using a bimolecular system consisting of a chromophore–acceptor diad (C^{2+}–A^{2+}) and an *N*-methylphenothiazine donor, we demonstrate that a ground-state association exists between the RuL_3^{2+} and the phenothiazine prior to photoexcitation. It is this association process that is responsible for the efficient CSS formation in the bimolecular system and, by inference, also must be an essential factor in the fully intramolecular process occurring with the D–C^{2+}–A^{2+} triad analogues.

Introduction

In photosynthetic reaction centers, nature has designed a molecular apparatus capable of separating charge with unsurpassed efficiency. In bacterial systems, where we have good structural data, the process initiates when a photon is absorbed by the so-called "special pair" of chlorophylls.[1,2] Within a few picoseconds, the resulting excited state transfers an electron with unity efficiency to an adjacent pheophytin electron acceptor, reducing it and leaving a hole on the special pair.[3] It is at this stage where arguably the most remarkable step in the entire photosynthetic process occurs. The photoinjected electron on the pheophytin has two choices. It can recombine with the hole on the special pair, or it can transfer to an adjacent quinone molecule that serves as a secondary electron acceptor. What makes this second step so surprising is that essentially 100% of the time the electron transfers to the quinone and does not recombine with the hole on the special pair, despite the much larger thermodynamic driving force for the latter process and roughly similar electron-transfer distances. Subsequently, the electron continues to cascade down the series of electron acceptors until eventually it and the hole are "harvested" as chemical energy.

Over the last several decades, various groups, including our own, have attempted to provide functional mimics of the first several steps in this photosynthetic process.[4–9] A common approach is to synthesize supramolecular assemblies that contain various functional analogues (which may or may not also be structural analogues) of the photosynthetic reaction center: for example, a light absorbing chromophore (C) covalently linked to an electron acceptor (A) and/or an electron donor (D). Efficiently mimicking the first step in the photosynthetic process is not difficult. There have been many systems reported over the years in which a photoexcited chromophore, attached to an acceptor (or a donor), undergoes electron-transfer quenching with essentially 100% efficiency. The tricky bit is efficiently affecting the second electron transfer which actually separates the charge. Here, success with synthetic mimics has been much less common because of the inherent competition between the productive, second charge separation step and the parasitic back electron transfer, wherein the latter usually wins. For example, it is uncommon for such systems to form multistep charge separated states (CSS) with quantum efficiencies, Φ_{CSS}, greater than ca. 25–30%, and frequently it is much lower. There are few examples outside the systems exemplified by the structure in Figure 1 (vide infra) where Φ_{CSS} is very large (e.g., >90%), but these systems are exceptions rather than the rule.[10]

A significant portion of our efforts in this area has focused on so-called "triad" assemblies incorporating an electron acceptor (A), an electron donor (D), and a light absorbing

(1) Deisenhofer, J.; Michel, H. *Annu. Rev. Cell Biol.* **1991**, *7*, 1−23.
(2) Deisenhofer, J.; Michel, H. *Annu. Rev. Biophys. Biophys. Chem.* **1991**, *20*, 247−266.
(3) Greenfield, S. R.; Wasielewski, M. R. *Photosynth. Res.* **1996**, *48*, 83−97.
(4) Kalyanasundaram, K. *Photochemistry of Polypyridine and Porphyrin Complexes*; Academic Press: San Diego, CA, 1992.
(5) Schanze, K. S.; Walters, K. A. In *Organic and Inorganic Photochemistry*; Ramamurthy, V., Schanze, K. S., Eds.; Marcel Dekker: New York, 1998; Vol. 2, pp 75−127.
(6) Armaroli, N. *Photochem. Photobiol. Sci.* **2003**, *2*, 73−87.
(7) Scandola, F.; Chiorboli, C.; Indelli, M. T.; Rampi, M. T. In *Biological and Artificial Supermolecular Systems*; Wiley: Weinheim, 2003; Vol. 3, pp 337−403.
(8) Gust, D.; Moore, T. A.; Moore, A. L. *Acc. Chem. Res.* **2001**, *34*, 40−48.
(9) Gust, D.; Moore, T. A. *Porphyrin Handb.* **2000**, *8*, 153−190.
(10) Bahr, J. L.; Kuciauskas, D.; Liddell, P. A.; Moore, A. L.; Moore, T. A.; Gust, D. *Photochem. Photobiol.* **2000**, *72*, 598−611.
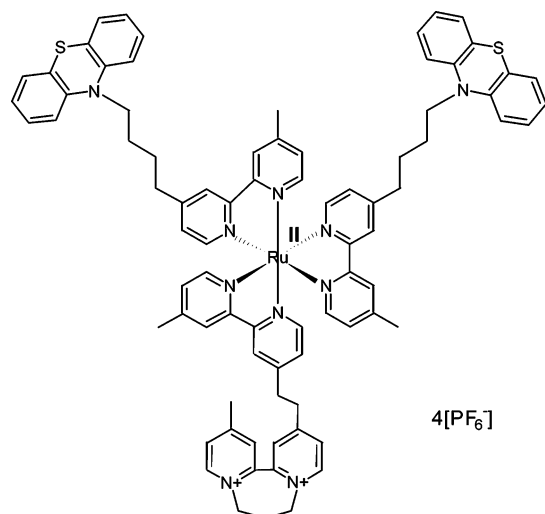
Figure 1. Representative donor−chromophore−acceptor triad complex that undergoes efficient photoinduced charge separated state formation.

chromophore (C) represented by the structure shown in Figure 1. The components of these triads typically consist of a central trisbipyridine ruthenium(II) chromophore ($RuL_3^{2+} = C^{2+}$) covalently linked to one or more phenothiazine donors (PTZ = D) and to an *N,N′*-diquaternary-2,2′-bipyridinium electron acceptor ($DQ^{2+} = A^{2+}$).[11−14] The linkages between the chromophore and the D and A^{2+} moieties are typically polymethylene chains emanating from the periphery of bipyridine ligands. Thus, the saturated alkyl chains bridging the molecular components are both nominally electrically insulating and flexible. The molecule shown in Figure 1 is one example of roughly 50 similar triad assemblies that we have prepared and studied.[11−14]

Considering the many types of light-induced charge separation systems that exist, there is no a priori reason one should expect triads exemplified by Figure 1 to be uniformly efficient at charge separation; yet, they are. Typically, all $D−C^{2+}−A^{2+}$ systems of this family undergo photoinduced CSS formation with very high quantum efficiencies, *often approaching unity.*[15,16] Additionally, counter to what Marcus Theory predicts, there seems to be little correlation between the thermodynamic driving force for the various electron-transfer steps and Φ_{CSS}. To illustrate this point, consider the $D−C^{2+}−A^{2+}$ triad shown in Figure 1 but with two methylenes in the chain connecting the quaternary nitrogens of the acceptor (rather than three). The photoinduced CSS formed from this triad stores ca. 1.13 eV of energy, about 56% of the triplet metal-to-ligand charge-transfer excited state (^{3}MLCT) energy and 42% of the incident photon energy at λ_{max} of the chromophore absorption (460 nm). Altering the diquat acceptor such that a four-carbon chain links the two quaternary nitrogens increases the energy stored in the CSS to 1.47 eV or 72% ^{3}MLCT energy and 55% of the incident photon energy at

λ_{max}, yet both systems have essentially the same Φ_{CSS} (close to unity). For comparison, the group at the Center for Study of Early Events in Photosynthesis at Arizona State University has studied D−C−A triads containing carotenoid donors, porphyrin chromophores, and C_{60} acceptors. Within this family of triads, Φ_{CSS} can be changed from 100 to 22% by merely altering the type of substituents on the porphyrin chromophore periphery without even affecting the amount of stored energy.[10,17]

The purpose of this article is to develop an explanation for why the particular assemblies exemplified in Figure 1 are so uniformly efficient at forming CSS while other putatively similar photoinduced charge separation systems are not. Before embarking on the discussion of the present results, it is necessary to review a few important general facts established in previous studies about this family of triad assemblies. The excited-state form of the chromophore is a ^{3}MLCT that is highly luminescent in the absence of any attached acceptors or donors. The solution emission lifetime, τ_{em}, is ca. 600 to 900 ns dependent upon the solvent. Diad assemblies of both $C^{2+}−A^{2+}$ and $C^{2+}−D$ have been prepared and their emission lifetimes examined to establish the respective quenching rates. As the driving force is changed and numbers of methylenes in the chain linking C^{2+} and A^{2+} are varied from 2 to 6, the oxidative electron-transfer quenching rates for $C^{2+}−A^{2+}$ diads vary from about 1×10^{10} to 1×10^7 s^{-1}.[12,14,18−20] In contrast, as the number of methylenes in the chain linking C^{2+} and D is varied from 1 to 9, the reductive quenching rates for $C^{2+}−D$ vary only from ca. 5×10^6 to 1×10^6 s^{-1}.[13,21] Thus, the slowest oxidative quenching is at least 2 times faster than the fastest reductive quenching. More importantly, when the emission decay rate of *any* $D−C^{2+}−A^{2+}$ triad is compared with that of the corresponding $C^{2+}−A^{2+}$ diad (i.e., with the same A^{2+}-containing ligand), the *relative rates* never differ by more than a factor of 2 even though the absolute decay rates change by more than a factor of ca. 10^3 (over the entire collection of compounds). The conclusion that must be drawn from these data is that the initial quenching event in all $D−C^{2+}−A^{2+}$ triads of this family is *always* oxidative quenching and D is, at this point, not involved:

$$D−C^{2+}*−A^{2+} \rightarrow D−C^{3+}−A^{•+}$$
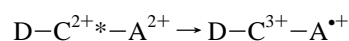
Another relevant fact from these earlier studies is that, in the time-resolved absorption spectra of the $C^{2+}−A^{2+}$ diads, there is never any detectable amount of $A^{•+}$ present.[12] One must conclude then, that the back electron transfer rate for

$$C^{3+}−A^{•+} \rightarrow C^{2+}−A^{2+}$$
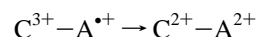
must be significantly faster than the oxidative quenching rate.

At this juncture, the stage has been set to propose two alternate hypotheses for the origin of the consistently large Φ_{CSS} values of these triads:

(11) Danielson, E.; Elliott, C. M.; Merkert, J. W.; Meyer, T. J. *J. Am. Chem. Soc.* **1987**, *109*, 2519−2520.

(12) Cooley, L. F.; Larson, S. L.; Elliott, C. M.; Kelley, D. F. *J. Phys. Chem.* **1991**, *95*, 10694−10700.

(13) Larson, S. L. Ph.D. Dissertation, Colorado State University, Fort Collins, CO, 1994.

(14) Larson, S. L.; Elliott, C. M.; Kelley, D. F. *J. Phys. Chem.* **1995**, *99*, 6530−6539.

(15) Klumpp, T.; Linsenmann, M.; Larson, S. L.; Limoges, B. R.; Buerssner, D.; Krissinel, E. B.; Elliott, C. M.; Steiner, U. E. *J. Am. Chem. Soc.* **1999**, *121*, 4092.

(16) Klumpp, T.; Linsenmann, M.; Larson, S. L.; Limoges, B. R.; Buerssner, D.; Krissinel, E. B.; Elliott, C. M.; Steiner, U. E. *J. Am. Chem. Soc.* **1999**, *121*, 1076−1087.

(17) Kodis, G.; Liddell, P. A.; Moore, A. L.; Moore, T. A.; Gust, D. *J. Phys. Org. Chem.* **2004**, *17*, 724−734.

(18) Schmehl, R. H.; Ryu, C. K.; Elliott, C. M.; Headford, C. L. E.; Ferrere, S. *Adv. Chem. Ser.* **1990**, *226*, 211−223.

(19) Cooley, L. F.; Headford, C. E. L.; Elliott, C. M.; Kelley, D. F. *J. Am. Chem. Soc.* **1988**, *110*, 6673−6682.

(20) Ryu, C. K.; Wang, R.; Schmehl, R. H.; Ferrere, S.; Ludwikow, M.; Merkert, J. W.; Headford, C. E. L.; Elliott, C. M. *J. Am. Chem. Soc.* **1992**, *114*, 430−438.

(21) Larson, S. L.; Elliott, C. M.; Kelley, D. F. *Inorg. Chem.* **1996**, *35*, 2070−2076.
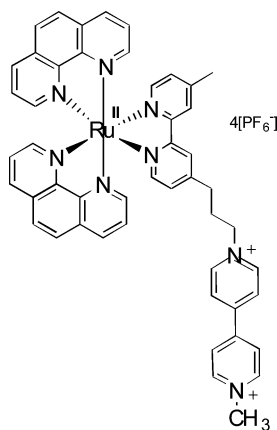
Figure 2. $C^{2+}-A^{2+}$ diad, **VI**, used in bimolecular quenching experiments with *N*-MePTZ donor.

1. The rate of intramolecular electron transfer between D and C^{3+} is inherently and significantly faster than that between C^{3+} and $A^{\bullet+}$, and there is nothing else unusual about these triads.

2. The rate of intramolecular electron transfer between D and C^{3+} is abnormally fast as a result of some type of ground-state association involving D prior to photoexcitation.

To test these hypotheses, it is necessary to determine the effect on Φ_{CSS} of varying the relative concentrations of D and C. Obviously, this cannot be done in an entirely intramolecular system. Thus, in what follows, results are presented for the CSS process in a bimolecular system consisting of an *N*-methylphenothiazine (*N*-MePTZ) donor, D, and a $C^{2+}-A^{2+}$ diad. Figure 2 shows the $C^{2+}-A^{2+}$ moiety, **VI**, chosen for the present study. The C^{2+} and A^{2+} components differ somewhat from those comprising the $D-C^{2+}-A^{2+}$ assemblies represented in Figure 1. First, the electron acceptor is a "paraquat-type" moiety rather than a "diquat" (i.e., it is based on an *N*,*N*′-dialkyl-4,4′-bipyridinium instead of an *N*,*N*′-dialkyl-2,2′-bipyridinium).[22] Second, the two "remote" ligands on the ruthenium (i.e., the ones not having an appended paraquat) are 1,10-phenanthroline rather than 2,2′-bipyridine. Phenanthroline was chosen over bipyridine for reasons that will be considered later but, suffice it so say that, from the ruthenium's perspective, the electronic difference between phenanthroline and bipyridine is fairly minor (i.e., $Ru(bpy)_3^{2+}$ and $Ru(phen)_3^{2+}$ have very similar visible spectra and redox properties).[23] Regardless of the exact identity of the acceptor (i.e., whether diquat or paraquat), the first electron-transfer event following photoexcitation is oxidative quenching.[14,19,20] Paraquat was chosen as the acceptor on the basis of the recombination kinetics of this initial electron-transfer quenching product (vide infra).[18,22]

The choice of donor is straightforward. The redox potentials of *N*-alkylphenothiazines are essentially insensitive to the identity of the alkyl group. A methyl group is the least sterically demanding, and therefore *N*-MePTZ was employed as the donor.

Experimental Section

Syntheses. Unless otherwise stated, all chemicals were obtained from Aldrich and used without further purification. 4,4′-Dimethyl-2,2′-bipyridine (DMB) was purchased from Reilley Industries and recrystal-lized from ethyl acetate. Lithium diisopropylamid (LDA) was prepared by the addition of a heptane solution of *n*-butyllithium to diisopropyl-amine in tetrahydrofuran (THF). THF was dried by refluxing under nitrogen over sodium/benzophenone.

4-(3-Hydroxypropyl)-4′-methyl-2,2′-bipyridine, (I). Under nitro-gen, 0.95 equiv of LDA in THF was added to 10.0 g of DMB which had been dissolved in 200 mL of THF and cooled to −78 °C. This solution was stirred for 3 h. A 4-fold excess of ethylene oxide was then added via cannula. The reaction mixture was allowed to warm to room temperature and stirred for 18 h before quenching by addition of 100 mL of water. The THF was removed by rotary evaporation, and the product, 4-(3-hydroxypropyl)-4′-methyl-2,2′-bipyridine, was ex-tracted into methylene chloride (100 mL; 3×) from the aqueous slurry. The methylene chloride fractions were combined and brought to dryness by rotary evaporation. The solid residue was redissolved in ca. 150 mL of ethyl acetate and cooled to 0 °C, whereupon much of the unreacted DMB precipitated from solution while the product remained dissolved. Ethyl acetate was removed by rotary evaporation at room temperature, yielding the product contaminated with DMB. This crude product was purified by "flash" silica gel chromatography, eluting first with 10% ethyl acetate in methylene chloride until all DMB was off the column. The product was then eluted from the column by gradually increasing the mobile phase polarity by changing the ethyl acetate/methylene chloride ratio. After rotary evaporation of solvent, the remaining white solid, **I**, was vacuum-dried overnight to yield 5.1 g of product (41%); ^{1}H NMR (CDCl$_3$) δ −CH$_2$− 1.9 (quintet), CH$_3$ 2.4 (s), −CH$_2$− 2.8 (t), −CH$_2$OH 3.7 (t), aromatic 7.2, 8.3, 8.6.

4-(3-Bromopropyl)-4′-methyl-2,2′-bipyridine, (II). 4-(3-Hydroxy-propyl)-4′-methyl-2,2′-bipyridine was converted to **II** by refluxing for 12 h in a 1:1 mixture of aqueous HBr (48%) and acetic acid. The reaction mixture was cooled, and the pH was brought into the range of 5−6 by addition of aqueous sodium bicarbonate. The product was extracted into methylene chloride, which was then dried over magne-sium sulfate and filtered. The solvent was removed by rotary evapora-tion at room temperature, yielding a red oil (88%); ^{1}H NMR (CDCl$_3$) δ −CH$_2$− 2.2 (quintet), CH$_3$ 2.4 (s), −CH$_2$− 2.8 (t), −CH$_2$Br 3.4 (t), aromatic 7.2, 8.3, 8.6.

[1-Methyl-4,4′-bipyridinium](PF$_6$), (III). 4,4′-Bipyridine was stirred with a 2-fold excess of iodomethane in ether for 24 h in the dark. The resulting yellow precipitate, [1-methyl-4,4′-bipyridinium] iodide, was filtered and washed with cold ether. Dissolving the iodide salt in water and adding a saturated aqueous solution of ammonium hexafluoro-phosphate dropwise yielded the hexafluorophosphate salt as a white precipitate. The precipitate, **III**, was washed with cold water and vacuum-dried (28%); ^{1}H NMR (CD$_3$CN) δ CH$_3$ 4.4 (s), aromatic 7.8, 8.4, 8.8, 8.9.

[1-(3-(4′-Methyl-2,2′-bipyridin-4-yl)propyl)-1′-methyl-4,4′-bipy-ridinediium](PF$_6$)$_2$, (IV). Quantities of 0.5 g of 4-(3-bromopropyl)-4′-methyl-2,2′-bipyridine and 3.3 g (6 equiv) of [1-methyl-4,4′-bipyridinium](PF$_6$), **III**, were refluxed in 150 mL of butyronitrile under nitrogen, excluding light, for 24 h. The yellow precipitate was metathesized to the hexafluorophosphate salt by the procedure described earlier. Yield of 0.54 g (46%); ^{1}H NMR (CD$_3$CN) δ −CH$_2$−, CH$_3$ 2.4 (quintet + s), −CH$_2$− 2.9 (t), N⁺CH$_3$ 4.4 (s), N⁺CH$_2$ 4.7 (t), aromatic 7.2−8.9.

Ru(1,10-phenanthroline)$_2$Cl$_2$, (V). A quantitiy of 1.0 g of Ru-(DMSO)$_4$Cl$_2$[24] was dissolved in 25 mL of dimethylformamide which was previously dried over alumina. This solution was saturated with lithium chloride before adding 0.82 g (2 equiv) of 1,10-phenanthroline. The reaction mixture was warmed to just below reflux and stirred for 1 h. Additional lithium chloride was then added, and the temperature increased to full reflux. After 75 min of being refluxed, the solution was cooled to room temperature and 60 mL of water was added. The

(22) Yonemoto, E. H.; Riley, R. L.; Kim, Y. I.; Atherton, S. J.; Schmehl, R. H.; Mallouk, T. E. *J. Am. Chem. Soc.* **1992**, *114*, 8081−8087.
(23) Balzani, V.; Juris, A.; Barigelletti, F.; Campagna, S.; Belser, P.; von Zelewsky, A. *Coord. Chem. Rev.* **1988**, *84*, 85−277.

(24) Wilkinson, G.; Evans, I. P.; Spencer, A. *J. Chem. Soc., Dalton Trans.* **1973**, 204−209.

precipitated crude product, **V**, was filtered and vacuum-dried (17%) and used in subsequent reactions without further purification; ^{1}H NMR (CD$_3$CN) δ CH$_3$ 2.5 (s), aromatic 7.1−8.7.

[Ru(1,10-phenanthroline)$_2$(4-(3-(1′-methyl-4,4′-bipyridinediium-1-yl)-propyl)-4′-methyl-2,2′-bipyridine)](PF$_6$)$_4$, (VI). Quantities of 79 mg of Ru(phen)$_2$Cl$_2$ and 100 mg (1 equiv) of [1-(3-(4′-methyl-2,2′-bipyridin-4-yl)propyl)-1′-methyl-4,4′-bipyrinediium](PF$_6$)$_2$, **IV**, were refluxed in methanol for 18 h. The reaction vessel was kept in the dark under nitrogen for the duration of the reaction. Upon being cooled to room temperature, a precipitate formed that was filtered off and discarded. A solution of methanol saturated with ammonium hexafluorophosphate was added dropwise to precipitate the crude product, **VI**, as the hexafluorophosphate salt. "Flash" silica gel chromatography was used to isolate the product. The "full strength" elution solvent was 50:40:10 water/acetonitrile/saturated aqueous KNO$_3$. A gradient elution with the mobile phase was required where the full strength elution solvent was diluted at each stage with 1:1 acetonitrile/water. The crude product was dissolved in neat acetonitrile and loaded on to approximately 5 in. of flash silica gel in a 1-in. diameter column. The column was eluted with progressively less dilute solvent starting with a 20-fold dilution and ending with "full strength". Fractions containing only the desired product (as determined by TLC) were combined, and the acetonitrile was removed by rotary evaporation at just above room temperature. The product was metathesized to the hexafluorophosphate salt, and the resulting precipitate was washed with water. Yield of 66 mg (30%); ^{1}H NMR (CD$_3$CN) δ −CH$_2$− 2.4 (quintet), CH$_3$ 2.5 (s), −CH$_2$− 2.9 (t), N$^+$CH$_3$ 4.4 (s), N$^+$CH$_2$ 4.7 (t), aromatic 7.1−8.9; GC/MS (ES$^+$) m/z calcd 1279.15, found 1279.00.

[Ru(1,10-phenanthroline)$_2$(4,4′-dimethyl-2,2′-bipyridine)]-(PF$_6$)$_2$, (VII). Quantities of 100 mg of **V** and 34 mg of DMB were dissolved in 25 mL of ethanol and brought to reflux for 20 h. Ethanol (15 mL) was removed by rotary evaporation before 30 mL of water was added. The product was metathesized to the hexafluorophosphate salt as described and recrystallized twice from methanol. Yield of 26 mg (25%); ^{1}H NMR (CD$_3$CN) δ CH$_3$ 2.5 (s), aromatic 7.1−8.7; GC/MS (ES$^+$) m/z calcd 791.14, found 791.07.

Preparation of Samples. Sample solutions were prepared in a dark room and kept from light until frozen for degassing. A stock solution of **VI** in dichloromethane (Aldrich, Spectro Grade) was prepared by adding solvent to a small amount of the solid complex until the absorbance at the maximum of the MLCT band monitored at 450 nm in a 1-cm cell was approximately 0.15 (ca. 10^{-5} M). The appropriate amount of solid *N*-MePTZ to obtain each concentration desired was weighed into vials, and 3 mL of stock solution of **VI** was added to each vial. Samples were then transferred to an optical cell constructed with a sidearm for freeze−pump−thaw (FPT) degassing, a Teflon valve, and a fitting for attachment to a vacuum line. Solution in the cell was transferred to the sidearm and frozen in liquid nitrogen. Each sample was FPT degassed several times until there was no evidence of outgassing upon thawing.

Transient Absorption Measurements. The initial amount of CSS formed was determined by transient absorption spectroscopy. The 355-nm tripled output of a Spectra-Physics Lab-190 Nd:YAG laser producing 8-ns pulses at 30 Hz with a power of approximately 2.0 W was used to pump Coumarin 450 dye in a Spectra-Physics PDL-3 dye laser. The dye laser output at 450 nm was used to excite the sample. Typical output powers were approximately 70 mW. Alternately, an Opotek OPA was used to provide the 450-nm excitation beam at powers of 50−55 mW. An Oriel 75 W xenon arc lamp was employed as a continuous probe source.

The reduced viologen acceptor radical has an absorbance maximum at 397 nm. Prior to passing the probe light through the sample, this wavelength was isolated from the xenon lamp's continuous output using a Johnson and Johnson monochromator. Subsequent to passing through the sample cell, the probe beam was collimated and then focused onto the entrance slit of a Jarrell Ash model 82-410 monochromator after

Scheme 1. Jablonsky Energy Level Diagram for Collisional (Left-Hand Branch) and Preassociation Mechanisms (Right-Hand Branch) for CSS Formation in a C^{2+}−A^{2+}/D Bimolecular System
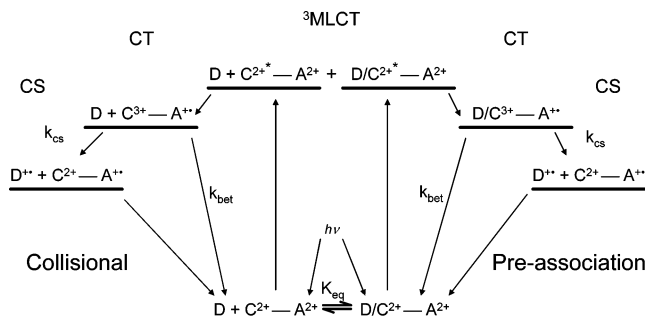
passing through a mechanical chopper operated at 30 Hz with slits such that light was transmitted about 3% of the time. For the Opotek OPA system, the chopper wheel was operated at 20 Hz. The input resistance of the oscilloscope was either 50 or 100 Ω. The photodiode output from the chopper was used as the trigger signal for the Nd:YAG laser. A Hamamatsu model R2496 photomultiplier tube (PMT) was employed to monitor the intensity of the probe beam. A Tektronix TDS 620B digital oscilloscope recorded the current output from the PMT for the first 500 ns following excitation by the pump beam. The oscilloscope was triggered with a Thorlabs DET210 fast photodiode. The results from 200 pulses were averaged. Differential absorbance due to the reduced viologen acceptor was calculated using Beer's Law.

Emission Lifetime Measurements. Emission lifetimes of **VI** in dichloromethane were obtained employing time correlation single photon counting as described by O'Connor and Phillips.[25] A Ti:sapphire regenerative amplifier (Coherent RegA) produced pulses centered at 866 nm with a 200 kHz repetition rate and 650 μJ/pulse. The light was frequency doubled to promote the MLCT transition. The subsequent fluorescence relaxation was collected through a subtractive double monochromator. Single photons impinging on a microchannel plate detector (Hamamatsu, MCP-PMT) were detected and digitized using an analog-to-digital converter (Oxford ADC) and served as the start pulse for a time-to-amplitude converter (Oxford, TAC). A small fraction of the excitation light was split off and directed to a fast photodiode (ThorLabs). This served as the stop pulse for the TAC. Signals from the TAC were fed into a multichannel analyzer (Oxford) whose output was monitored by a computer. Decay traces were collected until a sufficient signal-to-noise ratio was achieved to allow adequate data analysis.

Solution Viscosity Determination. Solution viscosities were measured using Cannon-Ubbelohde type viscometers from Cannon Instrument Company.

Results and Discussion

The first goal in this study is to establish which of the two hypotheses best explains the observed CSS formation in D−C^{2+}−A^{2+} assemblies. In the form of a Jablonsky diagram, Scheme 1 allows simultaneous examination of both of the limiting mechanistic possibilities.

The bottom center of Scheme 1 depicts a ground-state association equilibrium between the donor, D, and the C^{2+}−A^{2+} diad. For the sake of discussion, this association is represented in the scheme as if it were occurring between D and C^{2+}; however, the nature of any association has yet to be established and this issue will be revisited subsequently. In considering the two limiting cases represented by the left- and right-hand branches of Scheme 1, we assume that the CSS

(25) O'Connor, D. V.; Phillips, D. *Time-Correlated Single-Photon Counting*; Academic Press: London, 1984.
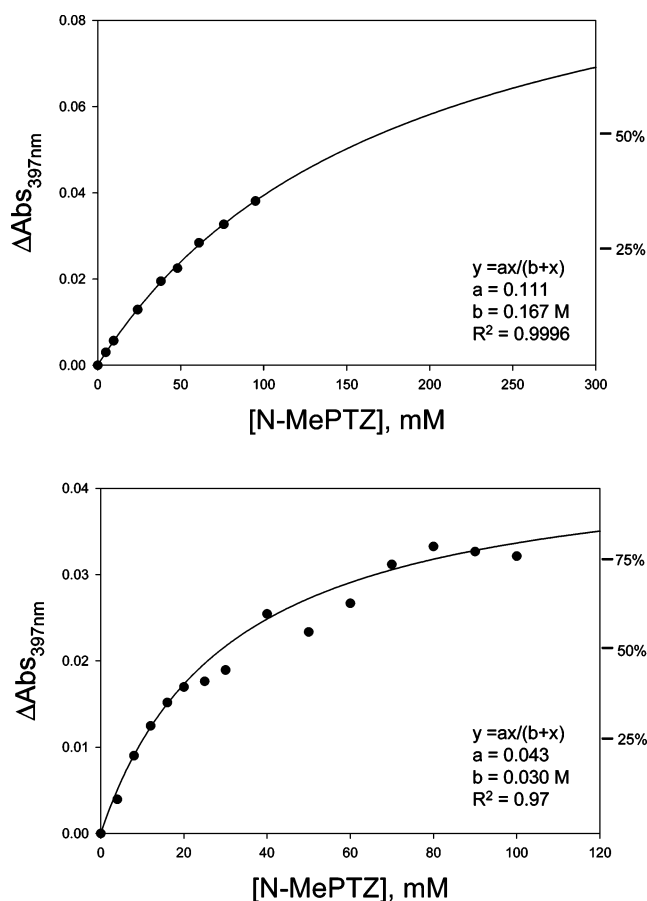
Figure 3. ΔA°_{397} (proportional to the amount of charge separated state initially formed) plotted vs [*N*-MePTZ] in acetonitrile (A) and dichloromethane (B) solvents. The right-hand *y* axis is the amount of CSS formed expressed as a percentage of CSS$_{max}$ as predicted from eq 3 (see text for explanation).

exclusively results through either a diffusional mechanism or a preassociation, not both.[26]

Transient spectroscopy was utilized to monitor the absorbance (397 nm) of the reduced viologen radical ($A^{\bullet+}$) formed upon photoexcitation (450 nm) of a $C^{2+}-A^{2+}$ diad as a function of [*N*-MePTZ]. First, in the absence of *N*-MePTZ there is no signal for reduced viologen. Thus, it can be assumed that the only viologen radical observed comes from CSS production. In other words, it is only when the donor reduces the oxidized chromophore prior to geminate recombination that the CSS (and thus reduced viologen) is observed. The lifetime of the bimolecular CSS is on the order of tens of microseconds. *Therefore, the change in absorbance at t → 0 (i.e., ΔA°_{397}) is directly proportional to the amount of CSS initially formed.*

The results obtained for CSS formation in acetonitrile and dichloromethane solvents are shown in Figure 3A,B, respectively, along with fits of the data to eq 3 (vide infra). While the range of [D] available in acetonitrile only permits about 40% of the predicted (from eq 3) maximum ΔA°_{397} (and, thus the maximum [CSS]) to be accessed, the quality of the fit is very good. The value of R^2 is 0.9996, which gives us considerable

confidence that the data in Figure 3A truly follow the functional form expressed in eq 3 (vide infra). In dichloromethane, it is possible to reach D concentrations yielding ΔA°_{397} values much closer to the maximum predicted from eq 3. As with acetonitrile, the fit at lower [D] to eq 3 is excellent, but above ca. 20 mM there is some scatter.[27] However, if only the data below 20 mM are used in the fit to eq 3, almost exactly the same values of *a* and *b* result (i.e., the fit constants) as when the entire data set is used.

In a mechanism involving only bimolecular diffusional encounters between the *N*-MePTZ donor and $C^{3+}-A^{\bullet+}$ (the left-hand side of Scheme 1), the resulting relationship connecting [CSS] and [D] takes the form:

$$\frac{[CSS]_0}{[CA]_i} = \frac{(k_{cs}/k_{bet})[D]}{1 + (k_{cs}/k_{bet})[D]} \tag{1}$$

where $[CA]_i$ is the total concentration of the $C^{2+}-A^{2+}$ diad, $[CSS]_0$ is the concentration of CSS at $t = 0$, k_{cs} is the bimolecular rate constant for forming the charge separated state, and k_{bet} is the rate of geminate recombination between $C^{3+}-A^{\bullet+}$ (Scheme 1).

If, on the other hand, ground-state association between D and $C^{2+}-A^{2+}$ was the sole mechanism responsible for CSS formation (the right-hand side of Scheme 1), the following relationship results:

$$\frac{[CSS]_0}{[CA]_i} = \frac{(k_{cs}/k_{bet})}{1 + (k_{cs}/k_{bet})} \cdot \frac{K_{eq}[D]}{1 + K_{eq}[D]} \tag{2}$$

where K_{eq} is the complexation equilibrium constant. Again, in deriving eq 2, it is assumed that an equilibrium association between D and $C^{2+}-A^{2+}$ is established prior to excitation and that CSS is only formed from that part of the total population of $C^{2+}-A^{2+}$ that is associated with D in the ground state. Additionally, k_{bet} and k_{cs} are, respectively, first-order rate constants of geminate recombination and charge separation relevant to the associated complex. In this instance, k_{bet} may or may not be the same as k_{bet} in the absence of $D/C^{2+}-A^{2+}$ association (i.e., as in eq 1).

In either of the above scenarios, the governing relation between $[CSS]_0$ and [D] has the same functional (i.e., mathematical) form. Also, since $[CSS]_0$ is directly proportional to ΔA°_{397}, both expressions can be written in the general form:

$$\Delta A^\circ_{397} = a\{[D]/(b + [D])\} \tag{3}$$

Thus, the only differentiating factors in the mathematical relations governing the two limiting mechanisms are the meaning of the constants. In both cases, the constant *a* depends on, among other things, experimental parameters such as the laser power and overlap of the pump and probe beams. For the sake of the work presented here, *a* can be considered to be an arbitrary constant in both models. In contrast, *b* is independent of similar experimental parameters (as long as they are constant). In the case of a simple bimolecular collisional reaction,

(26) It is also assumed that the extinction coefficient at 450 nm is the same for free $C^{2+}-A^{2+}$ and $D/C^{2+}-A^{2+}$. This assumption is necessary to assure that the same relative fractions $C^{2+}-A^{2+}$ and $D/C^{2+}-A^{2+}$ are excited as exist in the equilibrium solution. The validity of this assumption can be defended on the basis of the very minor change observed in the MLCT spectrum upon addition of *N*-MePTZ (see Figure 6).

(27) At the higher [D] there is moderate absorbance of *N*-MePTZ at 397 nm that lowers the signal-to-noise of the measurement and likely contributes to the scatter in ΔA_{397}. In comparing the data in Figure 3A,B, it is noteworthy that at a given [*N*-MePTZ], the [CSS] produced relative to the maximum amount predicted, [CSS]$_{max}$, differs significantly for the two solvents (see also Supporting Information).

$$b = k_{\text{bet}}/k_{\text{cs}} \tag{4}$$

In the case of an equilibrium preassociation,

$$b = K_{\text{eq}}^{-1} \tag{5}$$

Mallouk et al. previously reported values for both k_{et} and k_{bet} obtained in acetonitrile for a $C^{2+}-A^{2+}$ complex very similar to **VI**.[28] Values of the forward electron-transfer rate constant, k_{et}, for Mallouk's complex and for **VI** (in dichloromethane) are similar (1.9×10^9 and 8.2×10^{10} s^{-1}, respectively). It is reasonable to assume, therefore, that Mallouk et al.'s value of k_{bet} (6.5×10^9 s^{-1}) is a fair lower-limit estimate for the analogous process in **VI**. Assuming the bimolecular collisional mechanism and using Mallouk's value for k_{bet} and the value of b obtained from the fit to eq 3, a lower limit of 3.9×10^{10} M^{-1} s^{-1} is obtained for k_{cs}. Using the standard relation[29]

$$k_{\text{diff}} = \frac{8RT}{3\eta} \tag{6}$$

we calculated an estimate for the diffusion-controlled limiting rate constant of CSS formation in acetonitrile to be 2×10^{10} M^{-1} s^{-1}, where η is the viscosity of acetonitrile at room temperature. The lower limit for k_{cs} obtained from the fit to eq 3 is thus greater than the estimated diffusion controlled rate constant by a factor of ca. 2. The same calculations performed on the dichloromethane data yield a lower-limit value for k_{cs} of 2.1×10^{11} M^{-1} s^{-1}, and an estimated diffusion-controlled rate constant is 1.7×10^{10} M^{-1} s^{-1} (i.e., k_{cs} is too large by an order of magnitude). Both calculations depend on the assumption that Mallouk et al.'s value is a reasonable lower-limit estimate for k_{bet}.[30-32] The observations that (1) irrespective of solvent, we were unable to observe any photoreduced acceptor with **VI** in the absence of *N*-MePTZ and (2) back electron transfer rates for related compounds are typically not strongly solvent dependent are facts fully consistent with a $k_{\text{bet}} > 6.5 \times 10^9$ s^{-1} for **VI**.

The results that the values of k_{cs} exceed the diffusion-controlled limit in both solvents are strongly suggestive that the mechanism of CSS formation is not diffusional; however, a much stronger argument can be made by examining the dependence of Φ_{CSS} on solution viscosity. A series of stock solutions containing ca. 10^{-5} M $C^{2+}-A^{2+}$ complex (**VI**) and 50 mM *N*-MePTZ were prepared in dichloromethane solvent. To these solutions, 0–80 mg/mL of polystyrene was added to increase solution viscosities. A corresponding weight of toluene was also added such that the (polystyrene + toluene)/solvent ratio was held constant. The viscosity of each solution was measured five times, and the averages ranged from 0.46 to 12.1 cP. Figure 4 shows the dependence of ΔA°_{397} on viscosity.

These data demonstrate conclusively that the amount of $[\text{CSS}]_0$ formed is independent of solution viscosity. Clearly, a ca. 25-fold increase in viscosity with *no change* in $[\text{CSS}]_0$
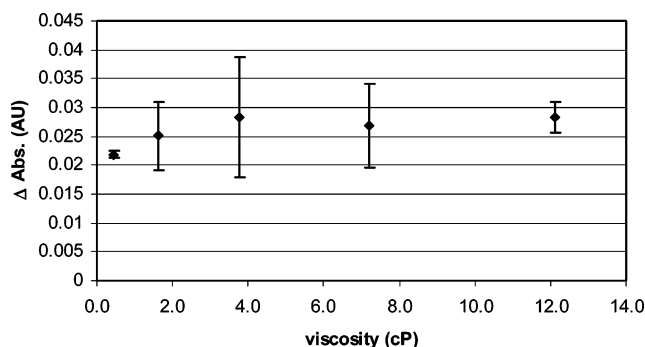
Figure 4. ΔA°_{397} (proportional to the amount of charge separated state initially formed) in the presence of 50 mM *N*-MePTZ plotted vs solution viscosity. The error bars represent one standard deviation.

effectively rules out any CSS formation mechanism whereby simple collisional encounters between D and $C^{3+}-A^{\bullet+}$ are involved (i.e., hypothesis 1). If the process is not collisional, then the only reasonable possibility remaining is the mechanism represented in the right-hand side of Scheme 1 and by hypothesis 2. However, none of the results considered thus far addresses the nature of the preassociation ground state. To shed light on this issue, other data must be considered.

In looking into the nature of the association, it is helpful at this point to construct two additional hypotheses:

2a. The association between D and $C^{2+}-A^{2+}$ leading to CSS formation is between D and C^{2+} (D/C^{2+}), most likely $\pi-\pi$ van der Waals in nature.

2b. The association between D and $C^{2+}-A^{2+}$ leading to CSS formation is between D and A^{2+} (D/A^{2+}), possibly both charge transfer and $\pi-\pi$ van der Waals in nature.

Distinguishing between these hypotheses has proven more challenging than simply demonstrating the participation of the preassociation in CSS formation. While there is literature precedent for both D/A^{2+}- and D/C-type associations (at least in loosely related systems),[33,34] there is no single piece of data that unambiguously demonstrates the nature of the association; rather, consideration of a collection of data from several experiments is necessary to develop a case. First, spectral evidence for any association between the two pairs of moieties (i.e., between D/A^{2+} and D/C^{2+}) was examined. Neither D nor A^{2+} absorbs light in the visible, but both absorb strongly in the UV. If any degree of interaction between these species were occurring in solution, some perturbation in UV spectra of the two moieties should be evident, especially if there is any charge-transfer nature to that interaction. Figure 5 shows that the absorption bands of the donor and acceptor are unperturbed by mixing the solutions. This is most clearly demonstrated by the fact that the spectrum resulting from the mathematical sum of the individual components exactly overlays the spectrum obtained from mixing the donor and acceptor solutions together (within experimental error).

In contrast to the data in Figure 5, there is a small but clear perturbation in the visible spectrum of combined solutions of D and C^{2+}. Attempts to quantify the intermolecular interaction via titration are complicated by overlap from the intense MLCT transitions and the weak nature of the optical signal resulting from the D/C^{2+} interaction; nevertheless, the qualitative effect

(28) Yonemoto, E. H.; Saupe, G. B.; Schmehl, R. H.; Hubig, S. M.; Riley, R. L.; Iverson, B. L.; Mallouk, T. E. *J. Am. Chem. Soc.* **1994**, *116*, 4786–4795.
(29) Atkins, P. W. *Physical Chemistry*, 5th ed.; W. H. Freeman: New York, 1994.
(30) Ohno, T.; Yoshimura, A.; Prasad, D. R.; Hoffman, M. Z. *J. Phys. Chem.* **1991**, *95*, 4723–4728.
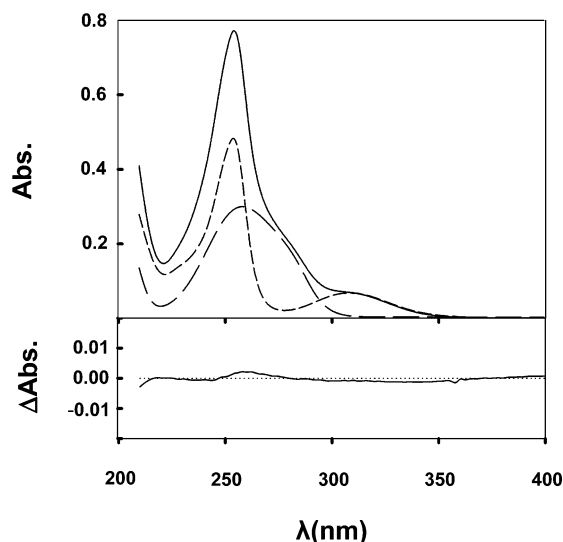(31) Sun, H.; Hoffman, M. Z. *J. Photochem. Photobiol., A* **1994**, *84*, 97–99.
(32) Linsenmann, M. Ph.D. Dissertation, University of Konstanz, Konstanz, Germany, 1997.

(33) Deronzier, A.; Essakalli, M. *J. Phys. Chem.* **1991**, *95*, 1737–1742.
(34) McClenaghan, N. D.; Loiseau, F.; Puntoriero, F.; Serroni, S.; Campagna, S. *Chem. Commun.* **2001**, 2634–2635.

Figure 5. Visible spectra in acetonitrile of a 1.5 mM solution of *N*-MePTZ (long-dashed curve), 1.5 mM solution of methyl viologen (short-dashed curve), and a solution that is 1.5 mM in both *N*-MePTZ and methyl viologen (solid curve). Superimposed on the solid spectrum is the sum of the two dashed spectra (i.e., the spectra of the isolated components). The lower part of the figure is the difference spectrum obtained by subtracting each spectrum of the individual components from the spectrum of the mixture.
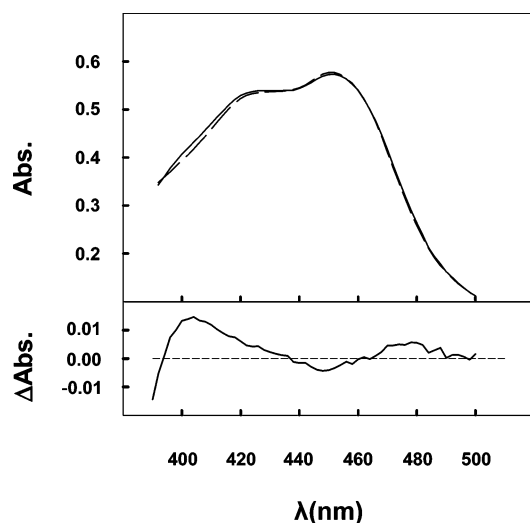
Figure 6. Visible spectra of a ca. 3×10^{-5} M solution of **VII** in dichloromethane (solid curve) and the same solution containing 50 mM *N*-MePTZ (dashed curve). The dashed curve was corrected for any small absorption of *N*-MePTZ by subtracting the spectrum of a 50 mM *N*-MePTZ solution in dichloromethane. The lower part of the figure is the difference spectrum obtained by subtraction of the dashed spectrum from the solid spectrum.

of added *N*-MePTZ on the MLCT band of **VII** can be clearly seen in the spectra of Figure 6. Similar evidence of a D/C^{2+} interaction comes from comparisons among spectra from D$-$C^{2+} diads, D$-$C$^{2+}-$A^{2+} triads, and isolated C^{2+}, D, and A^{2+} moieties. We have noted in earlier publications that, whenever a complex has incorporated one or more D-containing ligands, it is never possible to exactly simulate the spectrum by summing weighted spectra of the respective C^{2+}, D, and A^{2+} components.[13,21] Difference spectra from those attempts look qualitatively similar to those in Figure 6.[35]

(35) Limoges, B. Ph.D. Dissertation, Colorado State University, Fort Collins, CO, 2001.
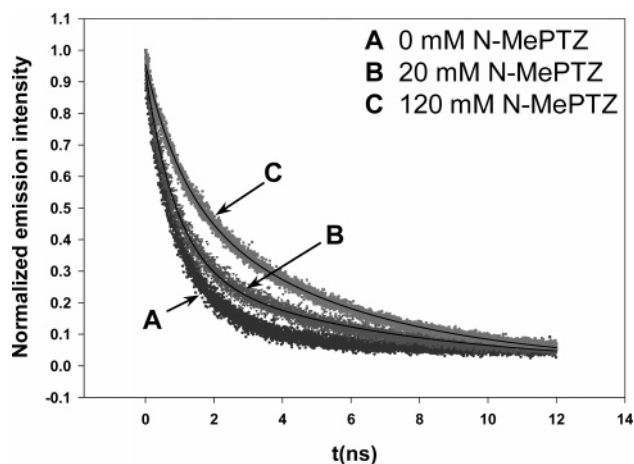
Figure 7. Time-resolved emission decays for a ca. 1×10^{-5} M solution of **VI** in oxygen-free dichloromethane.

Time-resolved emission spectra of C$^{2+}-$A^{2+} **VI** as a function of added *N*-MePTZ also assist in understanding the nature of the association between D and C$^{2+}-$A^{2+}. Figure 7 shows the emission decay of a ca. 1×10^{-5} M dichloromethane solution of **VI** in the presence of 0, 20, and 120 mM *N*-MePTZ, respectively. In the absence of any D, the lifetime of the emission is determined entirely by the oxidative quenching process. Obvious from the figure, however, is that addition of *N*-MePTZ *increases* the average emission lifetime of C$^{2+*}-$A^{2+}. From biexponential fits, curves B and C in Figure 7 each consist of the same two lifetime components (i.e., 3.8 ± 0.2 and 0.72 ± 0.03 ns). While the lifetimes are within a similar experimental error, the relative contributions of each are different. When the data in Figure 7 is compared with that in Figure 3B, an interesting and relevant correlation emerges. As stated previously, the right-hand *y* axis of Figure 3A,B represents the fraction of CSS formed relative to the theoretical maximum CSS. That axis also represents the fraction of the total C$^{2+}-$A^{2+} which is tied up as D/C$^{2+}-$A^{2+}. Expressed as percentages, at 20 and 120 mM *N*-MePTZ, respectively, 40 and 80% of the C$^{2+}-$A^{2+} is associated with D. From the fits of the data in Figure 7, the slow component contributes 45 and 70% to the total emission at 20 and 120 mM *N*-MePTZ, respectively. The correlation suggests that the slow component of the emission decay arises from the fraction of the C$^{2+}-$A^{2+} population associated with D. Since conformational flexibility of the C$^{2+}-$A^{2+} linkage appears to be required for the initial oxidative quenching,[18] were D associated with A^{2+} (rather than C^{2+}), much larger changes in emission lifetime should result than are observed. The difference in hydrodynamic radii between A^{2+} and D/A^{2+} should be large and should produce large changes in the quenching rate. In contrast, an association between C^{2+} and D might sterically restrict some encounters between A^{2+} and C^{2+} but only along a limited fraction of possible approach trajectories resulting in a more modest change in emission lifetime (as is observed).

Finally, if the association of D and C$^{2+}-$A^{2+} were between D and A^{2+}, the formation constant, K_{eq}, should be quite sensitive to the structure and redox potential of the acceptor. A titration with *N*-MePTZ in dichloromethane was carried out on an analogue of **IV** in which only the acceptor ligand was changed; specifically, the paraquat was replaced with the same diquat ligand as shown in Figure 1. Within experimental error, the

resulting titration is *identical* to that in Figure 3B (see Supporting Information; cf. Figures 3B and SM2). It is difficult, indeed, to rationalize how a K_{eq} for association between D and A^{2+} could be the same given such dramatic differences in A^{2+} structure (i.e., rigidly twisted versus freely rotating around the $\pi-\pi$ bond), especially in light of the strong solvent dependence demonstrated in Figure 3A,B.

To summarize, it seems quite clear from these collective results that CSS formation is dependent on a ground-state preassociation of the donor with the chromophore. Were there a significant charge-transfer component to this association process, differences in redox potentials would predict that a D/A^{2+} association should have a significantly more favorable enthalpy than would a D/C^{2+} association. If, on the other hand, the association is driven predominantly by van der Waals interactions and entropy, there is no a priori reason why one pairwise association should be favored over the other. The very minor changes in the absorption spectrum (Figure 6) and in time-resolved emission spectrum (Figure 7) produced by bimolecular association of *N*-MePTZ and **IV**, and the similarly small absorption and time-resolved emission differences between $C^{2+}-A^{2+}$ diads and $D-C^{2+}-A^{2+}$ triads,[12−14] all suggest that there is not a large enthalpic contribution for either the inter- or intramolecular association. The equilibrium may, therefore, be largely driven by entropy, but that is yet to be determined.

Finally, the question must be addressed of how the results from the bimolecular system actually inform about behavior in triad assemblies. First, consideration of molecular models demonstrates that intramolecular D/C^{2+} associations are sterically possible without significant strain energy. In the triad systems, the effective local concentration of D in the vicinity of the C^{2+} is much higher than can be achieved in the bimolecular system. This inherent concentration bias is the reason for using phenanthroline ligands, with their extended π-systems, in **IV** rather than bipyridines. The argument that an analogous intramolecular D/C^{2+} association occurs in the triad assemblies is further supported by the fact that difference spectra between $C^{2+}-A^{2+}$ diads and $D-C^{2+}-A^{2+}$ triads are qualitatively similar to the difference spectrum in Figure 6. Last, $D-C^{2+}-A^{2+}$ triads incorporating phenoxazine (POZ) rather than phenothiazine donors form photoinduced CSS with equivalently large Φ_{CSS} values. Two-dimensional $^{1}H-^{1}H$ ROESY NMR experiments performed on the POZ analogue of the $D-C^{2+}-A^{2+}$ triad shown in Figure 1 show clear evidence of spin exchange between the POZ and bipyridine protons, indicating their close average proximity as would be expected from the D/C^{2+} associations (see Supporting Information). Further, no cross-peaks are seen between the diquat acceptor and any species other than itself.

Conclusion

Scheme 2 represents, in cartoon form, how the D/C^{2+} association plays the critical role in intramolecular CSS formation for triads such as that in Figure 1. This mechanism provides a plausible explanation for the large CSS formation quantum efficiencies observed uniformly across this class of triads, but most importantly, it provides insight into a general means

Scheme 2. Depiction of the Phenothiazine Electron Donor Moiety Associated with the Local Bipyridine Ligand in a Triad Assembly Such as That in Figure 1
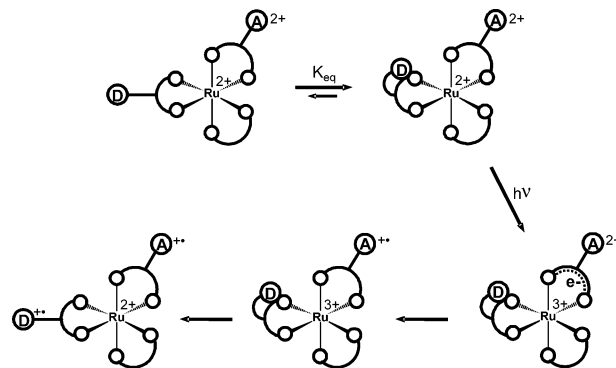
whereby systems might be designed to give efficient photoinduced charge separation *without automatically sacrificing the quantity of energy stored in the CSS*. Typically, the electronic coupling between donor and acceptor orbitals does not change dramatically upon electron transfer; consequently, an efficient forward electron transfer usually means an efficient recombination. Therefore, with a multistep photoinduced charge separation system, increasing Φ_{CSS} often comes with a concomitant cost in stored energy. For $D-C^{2+}-A^{2+}$ triads such as that in Figure 1, the flexible linkage allows D/C^{2+} to associate prior to any electron transfer, thus enhancing the D/C^{2+} orbital coupling, and to turn off the enhanced coupling by disassociation once the donor is oxidized (because of electrostatic repulsion; see Supporting Information for a more detailed consideration of this issue). Consequently, Φ_{CSS} is largely independent of driving force and, thus, of the energy stored in the CSS.

Considered in light of the present results, these specific triad assemblies provide the first example of which we are aware where a change in orbital coupling of this magnitude is induced by an intramolecular electron transfer, a change large enough to swamp the thermodynamic factors that usually control the charge separation kinetics. This suggests that related self-assembly processes could be intentionally designed and exploited to effect efficient CSS formation. Of particular importance is, in principle, that efficient photoinduced charge separation via such a mechanism should be possible without the loss in stored energy that most often accompanies efforts to use driving-force manipulations to improve CSS formation quantum efficiencies.

Supporting Information Available: 2D ROESY NMR spectra demonstrating correlation of the donor protons with the chromophore ligand protons as well as association data in mixed solvents and an analogous CA^{2+} with *N*-MePTZ system. This material is available free of charge via the Internet at http://pubs.acs.org.

JA0665500